https://doi.org/10.5194/egusphere-2024-2062
Preprint. Discussion started: 22 July 2024

New Particle Formation Events Observed during the COALA-2020 Campaign

Jhonathan Ramirez-Gamboa[1,2], Clare Paton-Walsh[1*], Melita Keywood[2], Ruhi Humphries[2], Asher Mouat[4], Jennifer Kaiser[4,5], Malcom Possell[3], Jack Simmons[1], Travis A. Naylor[1]

[1] Centre for Atmospheric Chemistry, School of Earth, Atmospheric and Life Sciences, University of Wollongong, NSW 2522, Australia

[2] Climate Science Centre, CSIRO Environment, Aspendale, VIC 3195, Australia

[3] School of Life and Environmental Sciences, University of Sydney, NSW 2006, Australia

[4] School of Civil and Environmental Engineering, Georgia Institute of Technology, Atlanta GA 30332, USA

[5] School of Earth and Atmospheric Sciences, Georgia Institute of Technology, Atlanta GA 30332, USA

* Correspondence: clarem@uow.edu.au

Abstract:

Aerosols play an important role in atmospheric processes influencing cloud formation, scattering and absorbing solar radiation, and as a part of the chemical reactions affecting the abundance of trace gases in the atmosphere. Ultimately aerosols affect the radiative balance of the earth modifying climate. A large fraction of aerosols is formed through chemical reactions following gas-to-particulate processes in the atmosphere: nucleation, condensation and growth. Biogenic Secondary Organic Aerosols (BSOA) are formed when plant produced volatile organic compounds (VOCs) react in the atmosphere through heterogeneous reactions. South-east Australia is one of the locations with the highest emissions of biogenic VOCs in the world, due to the high density of *Eucalyptus* species, which are high emitters of VOCs. The COALA-2020 (Characterizing Organics and Aerosol Loading over Australia) campaign worked towards a better understanding of biogenic VOCs in quasi-pristine conditions in the atmosphere and their role in particle formation.

The observations showed a highly reactive atmosphere with frequent new particle formation occurring (50% days with data) often associated with pollution plumes. Analysis of NPF events indicated that SO_2 and NOx plumes triggered particle formation, while particle growth depended on available VOCs, OH concentration (influenced by relative humidity), and the presence of multiple SO_2 and NOx intrusions promoted growth of smaller clusters. Nighttime NPF events correlated with NOx but the limited night-time data hindered conclusive interpretations. These findings highlight the significant role of biogenic VOCs, especially isoprene, in driving NPF and SOA formation in South-east Australia, even after major wildfires. The COALA-2020 campaign provided valuable insights into local atmospheric chemistry and its potential impact on regional air quality and climate. However, longer-term observations are crucial to understand seasonal variations, trends and extreme events.

Keywords: COALA-2020; aerosols, BVOCs, NPF.

1. Introduction

Aerosols can influence our health (Annesi-Maesano et al., 2013; Shi et al., 2016) but also play an important role in regulating Earth's energy balance, the hydrological cycle and even the abundance of key chemical species in the atmosphere such as hydroxyl (OH) and indirectly greenhouse gases (e.g., Kerminen et al.,

https://doi.org/10.5194/egusphere-2024-2062
Preprint. Discussion started: 22 July 2024

2012). The chemical composition, size and particle concentration determine the effects on health and the environment (Liu et al., 2016b; Pope and Dockery, 2006; Ren et al., 2017). Aerosols can be directly emitted (primary aerosols) or they can be product of interactions in the atmosphere (secondary aerosols) (Pöschl, 2005).

Secondary aerosols are produced via gas-to-particle transition, where reactive compounds in the atmosphere are oxidised to become low volatility organic compounds (LVOC). These compounds, along with sulfuric acid vapour are often involved in the nucleation process promoting clustering (e.g., Yu and Luo, 2009). Once the clusters (ultrafine particles) are formed, they can grow through coagulation and condensation potentially resulting in cloud condensation nuclei (CCN) (Dal Maso et al., 2005; Hussein et al., 2005; Kulmala et al., 2001). Usually, three distribution modes are used to classify the particle size distributions of ultrafine particles: the nucleation mode (<10 nm), the Aitken mode (10 - 100 nm) and the accumulation mode (> 100 nm). The formation of these molecular clusters and their subsequent growth to larger sizes is denominated new particle formation (NPF).

Biogenic VOCs play an important role in secondary organic aerosol (SOA) formation (e.g., Mahilang et al., 2021). Monoterpenes have higher SOA formation yields than isoprene (Friedman and Farmer, 2018; Riva et al., 2019; Zhang et al., 2018) but isoprene contributes more than half of the total BVOC emissions in the world making it an important SOA source too (e.g. Fry et al., 2018). Particularly the SOA yield of isoprene oxidised through NO_3 at night is reported to be several times the yield observed through the OH oxidation path (e.g. Ng et al., 2008). Recent studies suggest that in biogenic-rich regions isoprene-SOA yield can be much higher than previously reported when considering further oxidation of the products in low NO_x environments (e.g. Liu et al., 2016a), promoting the formation of key condensing species.

The OH availability in the atmosphere is key to promoting SOA formation (e.g. Song et al., 2019). To form key condensing species, multiple oxidation steps must happen to the original VOC molecule. After a VOC molecule oxidises becoming a more complex and larger OVOC, it is less likely to be oxidised again, particularly when in the presence of other VOCs with higher OH reactivity (Kiendler-Scharr et al., 2009). This was recently demonstrated in different chamber and ambient studies where isoprene mole fractions were many times higher than monoterpenes. In these studies, isoprene scavenged OH, interrupting the formation of C_{20} dimers and reducing the yield of highly oxygenated molecules (HOMs), thereby suppressing the nucleating process driving NPF (Heinritzi et al., 2020; Liu et al., 2016a). This effect is non-linear nor constant and will change with local conditions. High levels of SO_2 and VOCs in a humid atmosphere will enhance NPF (Nestorowicz et al., 2018; Song et al., 2019, p.20; Xu et al., 2021).

Understanding BVOC emissions and their role in SOA formation is important to accurately predict aerosol properties and their impact on climate. However, BVOC are poorly characterized under Australian conditions (Paton-Walsh et al., 2022). MEGAN emissions show south-east Australia as one of the BVOC hot-spots in the region (Guenther et al., 2012) but multiple modelling studies have shown that MEGAN emissions estimation might not be representing local conditions correctly in this region (Emmerson et al., 2016, 2018, 2019). Most of the Australian forested regions are dominated by high emitting *Eucalyptus* species (ABARES, 2019; Aydin et al., 2014; Padhy and Varshney, 2005) that combined with periods of temperature and drought stress create the conditions to have high emissions/concentrations of BVOCs in the atmosphere (Emmerson et al.,

https://doi.org/10.5194/egusphere-2024-2062
Preprint. Discussion started: 22 July 2024

2020; Fini et al., 2017; Ormeño et al., 2007). The emissions ratios of isoprene to other VOCs are poorly constrained and the local chemistry is not well understood.

The COALA-2020 campaign worked towards a better understanding of biogenic VOCs in quasi-pristine conditions in the atmosphere and their role in local atmospheric chemistry in south-east Australia. COALA-2020 was a collaborative effort between local institutions including the University of Wollongong, CSIRO, ANSTO, and the University of Sydney, and international peers from Georgia Institute of Technology, The University of California, Irvine, Nagoya University and Lancaster University. This part of the study focused on identifying and characterising NPF events after the "Black Summer" 2019-2020 Australian bushfire season. Here we aimed to identify drivers and conditions in which NPF started or were enhanced in the local environment.

2. Materials and Methods

2.1 The COALA-2020 Campaign

The COALA-2020 campaign took place at Cataract Scout camp (34°14'44" S, 150°49'26" E) located 20 km north-northwest of Wollongong on the east coast of NSW, Australia. The site is surrounded by a heavily forested area mainly stocked by Eucalyptus species (see Figure 1). North of the sampling site is the Appin Road, a four-lane arterial road connecting the M1 motorway on the east coast with south-western Sydney. Other possible anthropogenic sources impacting the site are two underground coal mine heads, the Appin Colliery (1.5 km to the northeast) and the West Cliff Colliery (2.5 km to the north). Besides the close sources it is important to note the proximity of the Sydney suburban area (around 18 km north-west), Sydney city (45 km north), Wollongong urban area and Port Kembla steelworks in the southern part of Wollongong (28 km to the southeast). The campaign was conducted from January 17th until March 23rd, 2020. The first period of the campaign was heavily impacted by smoke pollution from the bushfires affecting the region until February 5th, when a substantial rain event extinguished the fires and cleared the atmosphere of residual smoke pollution (Mouat et al., 2022; Simmons et al., 2022). This period was removed from the analysis presented here as we focus on understanding atmospheric processes during more normal conditions. Thus, this paper presents the analysis of BVOCs alongside anthropogenic emissions and their role

https://doi.org/10.5194/egusphere-2024-2062
Preprint. Discussion started: 22 July 2024

in NPF during *the second part of the COALA-2020 ambient measurements campaign running from February 5th until March 17th 2020.*

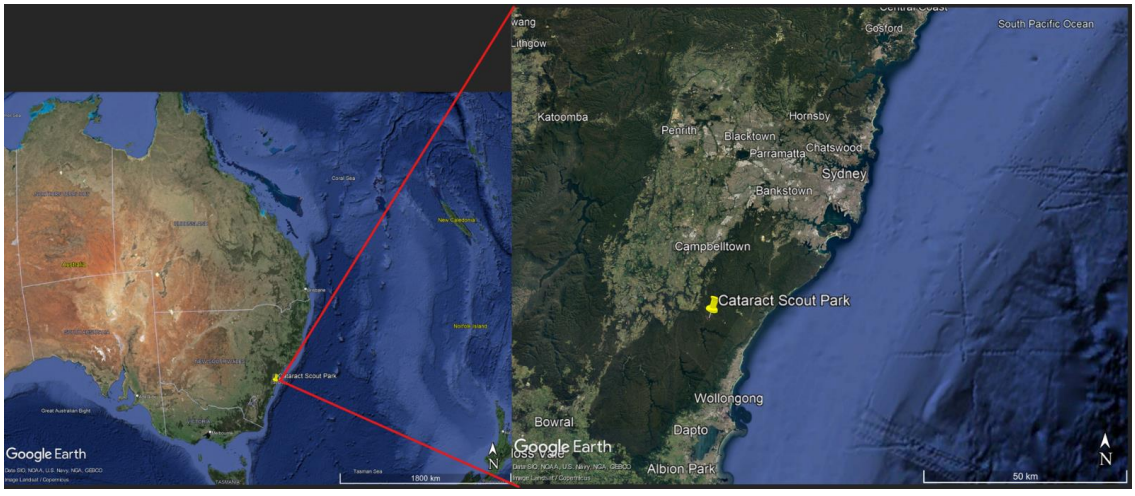

Figure 1 Location of the sampling site, to Sydney, NSW in the north. The sampling site had four different climate control containers for the instruments, as well as a soil sampling site around 50 meters northeast from the main sampling site and the High-Vol PM filter. Satellite view taken from Google Earth, © Google Earth 2024.

2.2 Instrumentation

The instruments deployed in the campaign are presented in **Table 1**. They included an air quality monitoring station owned and operated by the NSW Government Department of Climate Change, Energy, the Environment and Water (DCCEEW), located approximately 10m away from the main sampling line. This station included measurements of temperature, windspeed and direction, PM_{10}, $PM_{2.5}$, O_3, SO_2, NO_x, CO and visibility. All NSW air quality monitoring stations are accredited by the National Association of Testing Authorities (Australia). Inlet heights on this station were between 4.5m to 5.6 m above ground level.

VOCs were measured using a Proton Transfer Reaction Mass Spectrometer (Ionicon PTR-ToF-MS 4000) which operated with a mass range spanning m/z = 18-256. The drift tube was held at a temperature of 70° C, pressure at 2.60 mbar, and an electric field to molecular number density ratio of 120 Td. The instrument was housed in a separate climate-controlled unit. Samples were drawn from an inlet on a 10 m mast through a 20 m long PTFE line using a bypass flow of 1.2-3 L min^{-1}. Calibrations were made on site using standardized cylinders containing 17 compounds including isoprene, monoterpenes, methyl vinyl ketone (MVK) & methacrolein (MACR), benzene, C_8-aromatics, and C_9-benzenes (Mouat et al., 2022). Mass spectra were integrated to produce data at 1 minute temporal resolution. Mole fractions were further averaged on a five-minute basis.

A suite of aerosol instruments were operated within in the Atmospheric Integrated Research Facility for Boundaries and Oxidative eXperiment (AIRBOX) container (Chen et al., 2019). Sample air was drawn from a common aerosol bypass inlet. The inlet was located 5 m above ground level for the following instruments:

1. A Ultrafine Condensation Particle Counter (UCPC TSI 3776) was used to measure condensation nuclei number concentration greater than 3 nm (CN_3) (TSI Incorporated, Shoreview, MI, USA). The

https://doi.org/10.5194/egusphere-2024-2062
Preprint. Discussion started: 22 July 2024

instrument was operated at a sample flow rate of 300 mL min^{-1}. Measurements were recorded at 1 Hz temporal resolution.

2. A Scanning Mobility Particle Sizer (SMPS) was used to measure aerosol size distribution between 14 and 670 nm mobility diameter. Full scans of this size range were recorded every five minutes. The system consisted of an X-ray aerosol neutralizer and 3071 Long Electrostatic Classifier (TSI Incorporated, Shoreview, MI, USA) coupled to a 3772 CPC (TSI Incorporated, Shoreview, MI, USA). Sample was drawn from the same inlet as used by the UCPC.

3. Chemical composition of aerosols with diameter smaller than 1 µm (PM_1) were taken using a Time-of-Flight Aerosol Chemical Speciation Monitor (ACSM; Aerodyne Research Inc., Billerica, MA, USA). Mass concentrations of organics (Org), sulphate (SO_4^{2-}), nitrate (NO_3^-), ammonium (NH_4^+), and chloride (Cl^-) in the aerosol fraction 40-1000 nm vacuum aerodynamic diameter range, referred to as PM_1, are reported. Measurements were taken at 10-minute resolution. Sample air was drawn from the aerosol inlet common to the CPC and SMPS and dried using a Nafion dryer to < 40% relative humidity before sampling.

Table 1: Instruments deployed during the COALA 2020 campaign and included in the present analysis.

Name of parameter	Instrument type
NO - NO_2 -NO_x	API T204
O_3	Ecotech 9810
PM_{10}	Thermo (TEOM) 1405A
$PM_{2.5}$	Thermo (BAM)5014i
SO_2	API T100
Black Carbon	Magee Scientific Aethalometer AE33
VOCs	PTR-ToF-MS (Ionicon)
CO - CO_2 - CH_4 - N_2O	FTIR in situ analyser
CN_3	TSI 3776
Particle number size distribution (14 nm to 660 nm)	SMPS
PM_1 mass composition	Tof-ACSM, Aerodyne
Wind Speed and Wind Direction	2D Ultrasonic anemometer
Temperature, Relative humidity	Vaisala HMP155
Photosynthetic active radiation (PAR)	

2.3 NPF Classification Method

The method proposed by Dal Maso et al. (2005) was used to classify the particle size distribution data. To apply the method the particle number density plots were made for each day during the campaign. Then the plots were visually inspected to determinate if there was an event. A day of data was classified as an *event* if there was nucleation, meaning growth up to 25nm for at least two hours.

Once the events were classified, a logarithmic fit was applied to determine the geometrical diameter of each mode. The data was manually divided in chunks of 10 minutes to visually inspect and determine the number of modes and the geometrical diameter range of each event (nucleation <25nm, Aitken 25nm -100nm,

https://doi.org/10.5194/egusphere-2024-2062
Preprint. Discussion started: 22 July 2024

accumulation >100 nm). Once those parameters were defined and included in the code, each event was divided in periods of time with similar distribution modes.

For illustration a hypothetical event lasting two hours was divided in two: one hour with simultaneous two particle modes (nucleation and Aitken) and then one hour with just one particle mode (Aitken). This is done to estimate an accurate geometrical particle diameter based on the number of modes. This avoided the problems of changes in the number of modes in the sample. Finally, the data was merged again to have a time series of number of particles predicted with the fit, number of modes predicted and geometrical particle diameter.

The algorithm works by providing the number of modes observed in the input dataset. Then it selects the provided model equation for each mode number and iterates over a hundred fits looking for the best one. The Bayesian Information Criterion (BIC) was used to identify the best fit, looking for the lowest values. Once the best fit was selected, the total particle number estimated by the model was compared with the sample record for each sample to assure it was within a 5 % difference compared to the total particle number reported in the sample. The result was then visually checked looking for the geometrical diameter and how it compares to the distribution size plots from the raw aerosol distribution size data. Once the model was considered representative and accurate enough, the growth rate for each event was determined using a simple linear regression of the change in the geometrical diameter in time from nucleation to Aitken and eventually to accumulation mode.

3. Results and Discussion

3.1 Frequency of NPF Events

Of the forty days included in the analysis, fourteen (35%) showed clear NPF events, nine (22%) were considered undefined, eight (18%) didn't have enough data or were classified as a non-event and nine days (25%) didn't have any data. The percentage of days with NPF is similar to those of other sites in forested areas in the Northern Hemisphere (Kalkavouras et al., 2020; Uusitalo et al., 2021). On the days in which the particle growth pattern is not clear, the same chemical reactions driving the NPF events may also be influencing these particle clusters, but the pattern is obscured due to different factors influencing the chemistry and physically mixing the atmosphere. 35% of days with NPF events and 18% with undefined events implies a highly reactive atmosphere even in this rural area with relatively low anthropogenic influence.

3.2 Triggers for NPF Events

Of the fourteen days with NPF, five were registered during the night or early morning (before sunrise), and nine during the day. The starting time of the event was important to mark which possible reactions might be driving the oxidation of products that eventually nucleate. Besides that, the time series of SO_2, NO_x, ozone, VOCs and the aerosol composition were used to identify which variables influenced the aerosol formation and growth. Of the fourteen events, eight have VOC data and nine have aerosol composition data. Only three events led to accumulation sized particles (diameter >100 nm).

https://doi.org/10.5194/egusphere-2024-2062
Preprint. Discussion started: 22 July 2024

From the daily time series of all available variables, it is evident that SO_2 and NO_x are probably triggering or at least influencing the particle formation most of the time. As an example, the event on Feb 11th 2020, presented in Figure 2 shows how after there was a first SO_2 and NO_x peak coming to the site at around 8:00 am, one hour later the nucleation process starts. This event did not show a quick growth like several other events in the record possibly due to the early morning start time when there were not enough VOCs to accelerate the nucleation and growth process. Later, once the temperature starts to increase, enhancing the VOCs emitted, and there is more OH available in the atmosphere, there will be higher density of particles in both nucleation and Aitken mode. This difference is reflected in the peak of particles captured in the CN_3 data around 11:00 am.

https://doi.org/10.5194/egusphere-2024-2062
Preprint. Discussion started: 22 July 2024

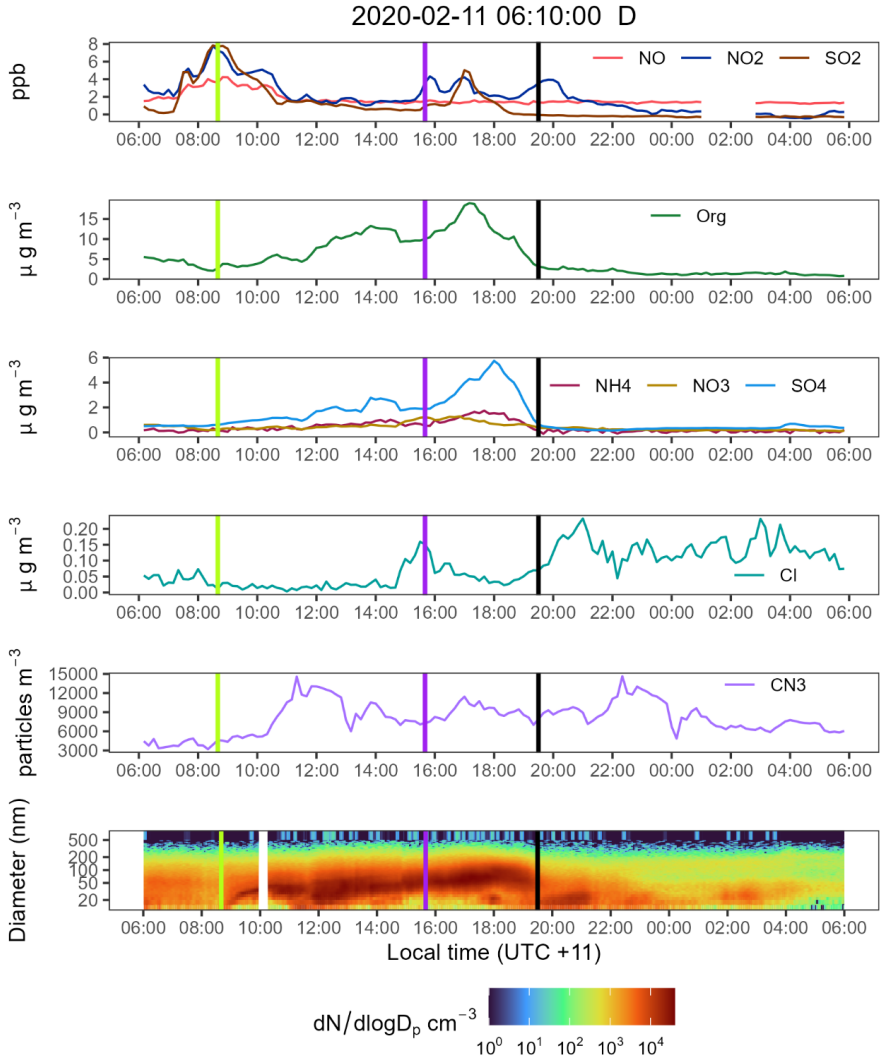

Figure 2 Time series for all selected variables during the NPF event during 2020-02-11. NO = Nitric oxide, NO2 = Nitrogen dioxide, SO2 = Sulphur dioxide, Org = Organic mass fraction, NH4 = Ammonium mass fraction, NO3 = Nitrates mass fraction, SO4 = Sulphates mass fraction, Cl = Chloride mass fraction, CN3 = Condensation Nuclei >3nm. VOCs mole fractions were not available during this specific event. Note how the fraction of organics, sulphates and ammonium increase with a positive correlation, dominating over the nitrate and chloride fractions until the end of the event. The light green vertical line marks the NPF approximated starting time. The purple line marks the time were subsequent SO_2 emissions impacted the site. The black line represents the NPF approximated ending time.

SO_2 appears to only affect daytime events, while NO_x seems to have a shared role in both daytime and night-time events. Trying to group the common factors influencing NPFs on daytime and night-time events, a

https://doi.org/10.5194/egusphere-2024-2062
Preprint. Discussion started: 22 July 2024

comparison of the growth rate was used to determinate if the rates were similar during the day and during the night.

3.3 Particle Growth Rates during daytime and nighttime events

The estimated growth rate is presented in Figure 3. Only four of the nine events during daytime (see upper panel of Figure 3) had a representative Pearson coefficient (R>0.6), the remaining five events did not have a stable linear growth and are not shown in the plot.

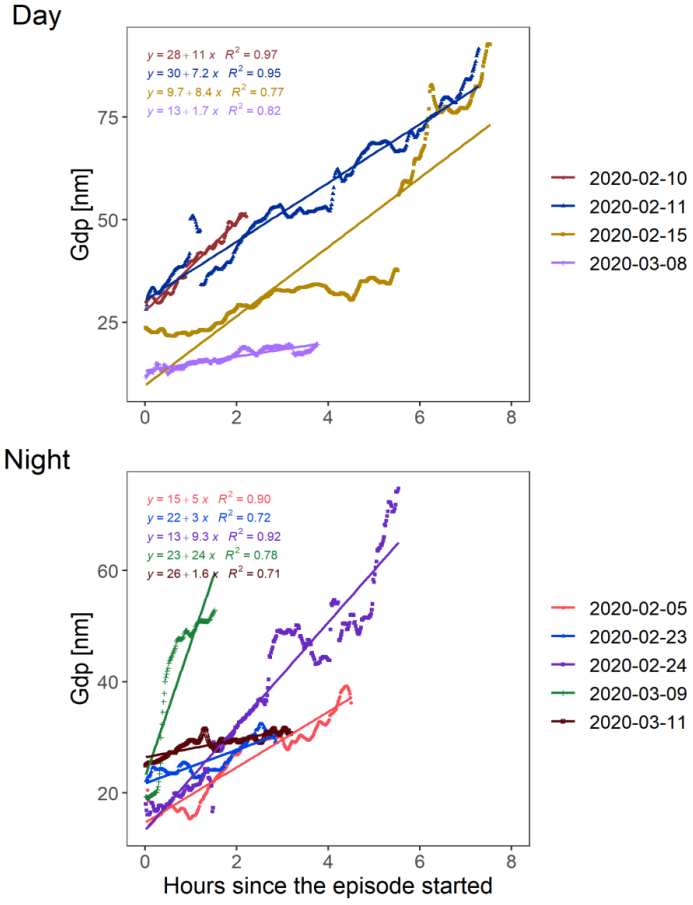

Figure 3: Geometric particle diameter evolution in each event where the logarithmic fit converged. The top panel presents the daytime data (only four events converged to a statistically significant model). The bottom panel presents the nighttime events.

During these more unstable events the influence of plumes on the sampling site bringing SO_2 and NO_x likely produced multiple reactions drastically changing the particle density in short periods of time or induced multiple formation events, making it harder to estimate the particle growth on these days using the same methodology. Event 2020-02-15 in Figure 3 is an example of how the geometric particle diameter can change

https://doi.org/10.5194/egusphere-2024-2062
Preprint. Discussion started: 22 July 2024

when there is rapid growth. The first part of the regression shows slower growth rate. After the 6th hour of slow growth, the rate increases substantially.

Some events showed how the daytime concentrations of SO_2 and NO_2 were so dynamic that it might prove difficult to study a particular phenomenon when sampling in the ambient air (see figure S1). Nonetheless, these events provide insight into the factors that may drive the growth and particle formation and so were included in all the analysis.

In contrast to the daytime events, all the night-time events were stable enough to determinate the event growth rate. The growth rate varied considerably between events (see lower panel of Figure 3) and most likely reflects differences in the factors driving the particle formation between these episodes. The differences in the growth rate might be directly affected by the main oxidation pathways available at the time of the reaction. These reactions pathways might include VOC oxidation through nitrates (NO_3^-) oxidation path during the night, leftover isoprene or monoterpene oxidation and condensation over previously formed clusters, oxygenated VOCs (OVOCs) brought to the site and condensed on formed seeds or starting nucleation, or VOC oxidation through the ozone pathway. Some of these processes were observed during the campaign and will be further explored on the nighttime events section.

3.4 Daytime NPF Events

From the timeseries analysis of all daytime events (see Figure 2, 5-8 and supplementary figures S1-S5), four key points were identified for NPF in the area:

1. SO_2 and NO_2 arriving at the site triggers nucleation and growth events.
2. VOC availability is needed for growth and nucleation.
3. The hours with VOCs and higher oxidation capacity in the atmosphere (OH concentrations are assumed to be higher during the hours with higher PAR will have the highest particle density and the highest frequency of the observed events.
4. There might be nucleation without SO_2 and NO_2 in the atmosphere but at a slower growth rate.

During most of the daytime events SO_2 and NO_2 plumes impacted the site at some stage of each event.

On some occasions the SO_2 plume might last for a couple hours as shown in the first part of the event on Feb 11th 2020 (see Figure 2), whilst at other times there were multiple peaks of high SO_2 measured at the site (Figures S2, S3, S4). Every time SO_2 was first detected at the site, some nucleation commenced within 0 to 150 minutes after the SO2 was first detected. This window of time matches the time needed to reach nucleation sized particles if we extrapolate the growth rate function from the daytime events previously discussed (see Figure 3). To highlight this phenomenon a cross correlation between SO_2 and the aerosol mass of SO_4 time series obtained from the tof-ACSM and the measured particle number concentration (CN_3) was applied. Figure 4 shows the Pearson correlation between SO_2 and the CN3 and SO4 in a window period of four hours i.e. starting two hours before the nucleation started and ending after the first two hours of the event. This time window aims to capture the SO_2 influence on the particle formation. Each line/point shows the correlations at 0, 30, 6, 90, 120 and 150 minutes lagged for each daytime event. The dotted blue lines show where the lagged correlation is significant at ($|r| > 0.5$).

https://doi.org/10.5194/egusphere-2024-2062
Preprint. Discussion started: 22 July 2024

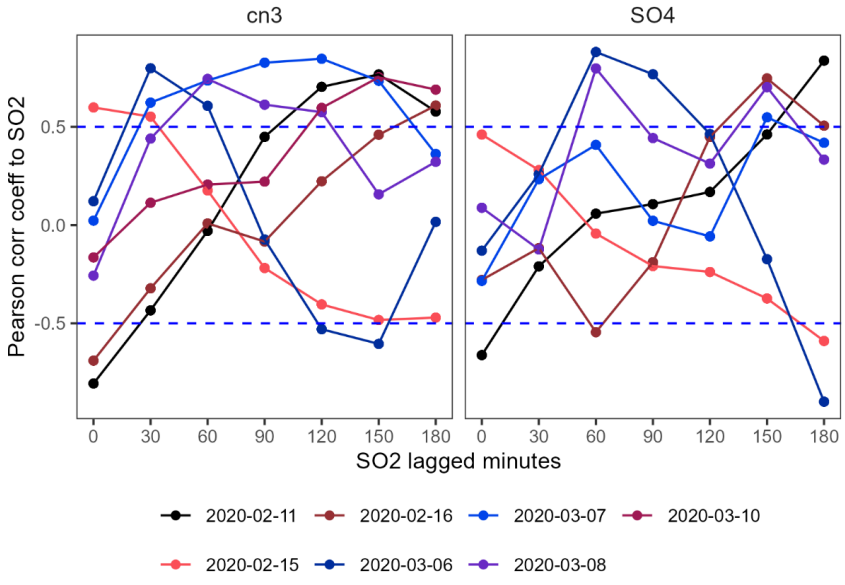

Figure 4 : Pearson correlation values obtained from the cross correlation between SO_2 and CN_3 and SO_4 mass. The dashed lines represent the 0.5 threshold as a reference to identify significant correlations. Events on Feb 10th and March 11th did not follow this pattern and were removed from the plot.

To interpret Figure 4, we can use the event on February 11th (black line) as an example. Here the correlation between SO_2 and CN_3 becomes significant (at $|r| > 0.5$) if the aerosol data is lagged 120 minutes and the correlation between SO_2 and SO_4^{2-} becomes significant after 3 hours. This means that if we move the SO_2 time series two hours forward it will be better correlated with the particle number concentration, accounting for the reaction time of SO_2 to produce SO_4^{2-} radicals and enhance/trigger the particle formation under the conditions in the atmosphere at the time. Usually, the SO_2 correlation with SO_4^{2-} takes longer to be significant. This is a potential indication of the order in which the chemical reactions happen. First, we will see oxidation of the SO_2 to SO_4^{2-} and then nucleation.

A similar result is observed for other events at different lagged times. The difference in the length of time necessary to achieve a significant correlation between SO_2 and the particle number seems to be related to the quantity of VOCs available after the SO_2 plume arrives at the site and how long the SO_2 is available in the atmosphere. Events on February 15th, March 06th and March 07th had the highest correlations in the first 30 minutes of lagging the SO_2 data. All these events had in common a relatively high isoprene mole fraction (>1 ppb) in the previous hour to the SO_2 coming to the site (see Figure S1, S2 and S5) or in the circumstances where VOC data were not available, conditions where isoprene mole fractions were assumed to be high (associated with weather conditions; i.e. high PAR and temperature see Figure S6). The event on March 8th also met this condition (see Figure S3), but the growth seems to be partially suppressed by other factors, as seen in the relatively low growth rate in Figure 4 compared to the other events.

https://doi.org/10.5194/egusphere-2024-2062
Preprint. Discussion started: 22 July 2024

The Feb 11th and Feb 16th events had similar arrival times for the SO_2 pollution (8:00 to 9:00) although the VOC mole fractions were too low to enhance the particle formation and growth. This presumption is supported by looking at the event on February 16th (see Figure S4). In this event, a first peak of SO_2 at 8:00 started some particle formation but subsequent SO_2 peaks at 10:00 and 12:00 (times where generally VOCs are higher) led to a NPF event that eventually grew to accumulation sized particles.

The event on March 10th shows how SO_2 pollution occurred around 10:00 when isoprene mole fractions are about 0.5 ppb promoting NPF. This event shows how even when VOCs available if there is no SO_2 in the atmosphere (13:00) the particle formation will substantially decrease, as shown in the CN_3 concentration (see Figure S7).

A similar result to SO_2 NPF events is observed when the cross correlation is applied with NO_2 data as shown in Figure 11. (Wang et al., 2019) reported an enhanced effect of SO_2 oxidation to SO_3^{2-} in the presence of NO_2 and H_2O. The resulting acidic aerosols can easily act as nuclei for VOC condensation explaining the correlations of SO_2 and NO_2 with the particle formation events (Wang et al., 2020a). These studies were made under urban-like conditions with high concentrations of SO_2 and NO_x to produce this effect. The atmospheric chemistry community is still debating the role of this reaction on SO_2 related aerosol formation, with recent experiments showing that the enhancement effect is not as large as originally proposed (Au Yang et al., 2018; Wang et al., 2020b). There are other reaction pathways that can lead to SO_3^{2-} formation such as SO_2 oxidation through the OH path (Long et al., 2017; Margitan, 1984) or photo-oxidation of SO_2 (Wang et al., 2020b). Nonetheless, measurements and experiments in rural atmospheric conditions provide insights into these phenomena a because of the multiple reactions happening depending on the atmospheric conditions at a given time.

https://doi.org/10.5194/egusphere-2024-2062
Preprint. Discussion started: 22 July 2024

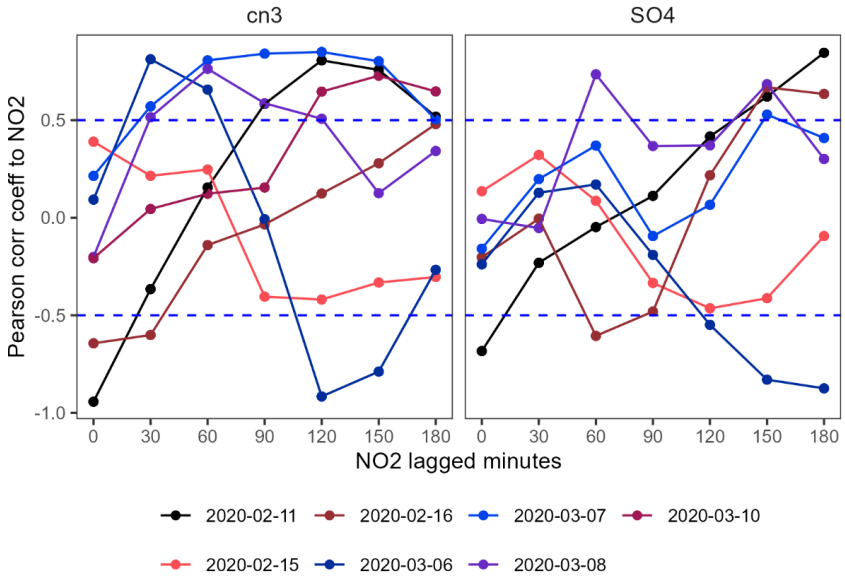

Figure 5: Pearson correlation values obtained from the cross correlation between NO_2 and CN_3 and SO_4 mass. The dashed lines represent the 0.5 threshold as a reference to identify significant correlations. Events on Feb 10th and March 11th did not fit into this category and were removed from the plot.

SO_2 and NO_2 are significantly correlated during most of the day-time events with a Pearson correlation of 0.78, suggesting a common source for both pollutants. The closest source of combustion products is the Appin Road located north of the sampling site. Given that the sampling site is away from other possible sources of SO_2 and NO_2 and the relatively low wind speeds during most of the campaign (see S8), combustion from mobile sources is considered the most likely source of both compounds. Another factor to contribute to this theory is that the SO_2 levels were higher during the day when most of the commuting takes place and leading to a higher vehicle density on the roads. The intermittent SO_2/NO_2 peaks suggest the influence of mobile sources with poor emission control onboard The effects of vehicles with poor emission control technologies on ambient concentrations of SO_2, NO_x, AVOCs and PM has been seen in different studies (Kari et al., 2019; Phillips et al., 2019; Smit et al., 2019) and the legislation controlling fuel standards and emissions is relatively lax in New South Wales (Paton-Walsh et al., 2019).

The availability of VOCs to react and produce oxygenated volatile compounds that might condense over the SO_4^{2-} seeds formed from SO_2 pollution impacting the site, is as important as the SO_2 presence and reaction. This has been previously reported by (Stangl et al., 2019), where chamber experiments showed that SO_2 presence can significantly enhance SOA formation from isoprene and monoterpene oxidation by ozone. (Xu et al., 2021) reported that water and SO_2 availability will change the role of SO_2 in the particle formation process. With high SO_2 mole fractions, the SO_2 reaction path will favour reaction to peroxides instead of stable Criegee intermediates, thereby enhancing particle growth, when the relative humidity is higher than 45%; a condition present during most of the COALA-2020 campaign. This suggests that under high SO_2, VOC

https://doi.org/10.5194/egusphere-2024-2062
Preprint. Discussion started: 22 July 2024

and relative humidity conditions, the particle formation and growth will occur. Such an effect was observed in some of the events, for example the event on February 16th (Figure S4). There was a continuous source of SO_2 impacting the site during this event in the period between 07:00 to 22:00. During the first half of the event (up to 14:00) organic aerosol mass fraction is almost as high as the sulphate mass, however after 14:00 there is an increase in the sulphate mass, which becomes the largest mass proportion of this event. The sulphate fraction is practically a mirrored version of the NO_2 and SO_2 lagged by an hour. The highest fraction of sulphates during this period can be explained by the previously mentioned effect of relative humidity, and VOCs.

As the night approaches, BVOC emissions decrease with temperature, leaving all existing VOCs to oxidize. This provides the initiation for further oxidation of OVOCs into more oxidized species, which are more likely to condense on existing particles. In addition, with the temperature decreasing the relative humidity increases, making this the ideal condition for particle growth, particularly sulphates. However, once the VOCs are mostly consumed (by around 22:00), there are insufficient VOCs to generate growth. This relationship is presented in Figure 6, where relative humidity and sulphate mass are positively correlated during the afternoon hours in the events which had multiple SO_2 peaks enhancing sulphate formation and particle growth.

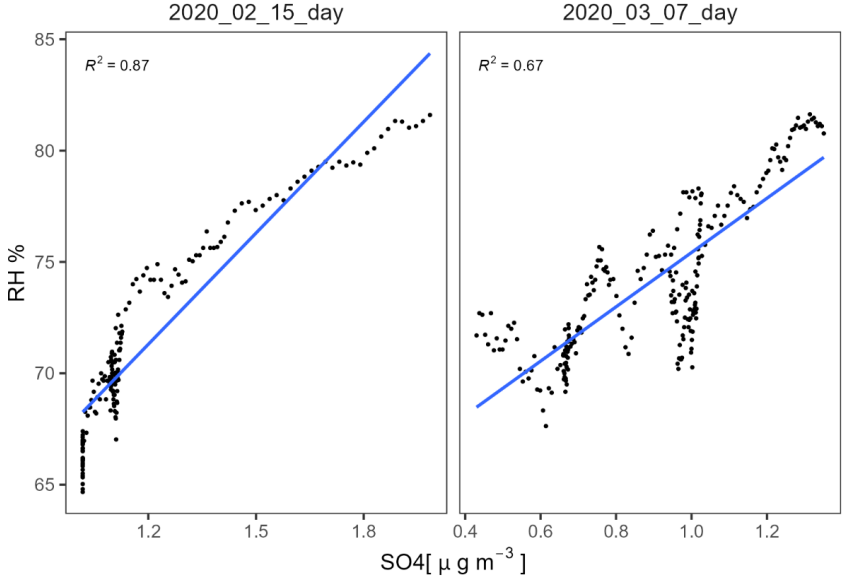

Figure 6: Scatter plot of the events on Feb 15th and March 7th comparing total sulphate mass against relative humidity in the afternoon hours (14:00 to 17:00).

The opposite conditions can also influence particle formation. When there is little SO_2 or NO_2 in the atmosphere but there are high enough VOC concentrations, there can be slow nucleation over time. Slow growth was observed during the February 10th event (Figure 7) and may be related to the condensation of monoterpenes oxidation products. Lab studies have shown that this process might take longer than other

https://doi.org/10.5194/egusphere-2024-2062
Preprint. Discussion started: 22 July 2024

particle formation processes because methacrolein (MACR) needs to be oxidized to produce aerosols (Kroll et al., 2006; Ng et al., 2006). Other processes such as autoxidation of monoterpenes could explain these events. Recently (Nie et al., 2023)) showed that low NO concentrations can enhance highly oxygenated molecules (HOMs) formation by favouring alkoxy radicals formation that are prone to autoxidise in pristine atmosphere or low-NO regimes.

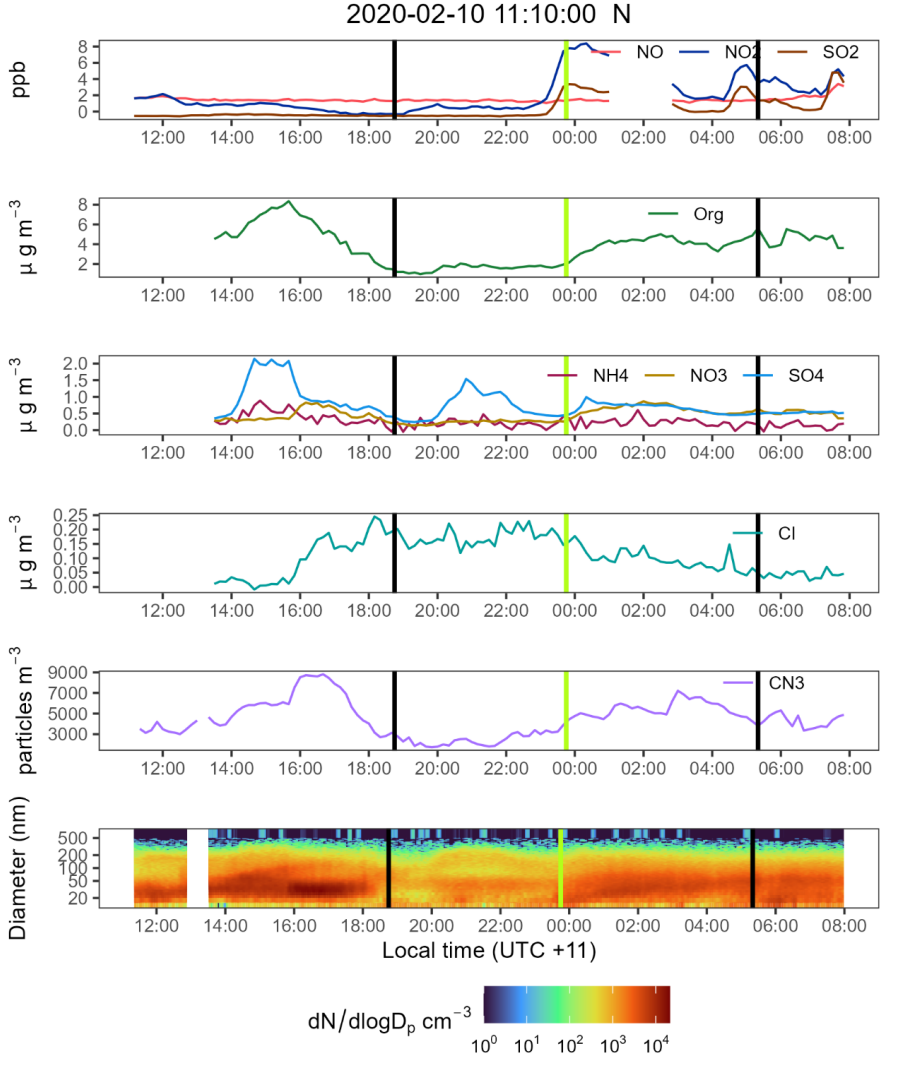

Figure 7: Time series of all selected variables during the NPF event during 2020-02-10. NO = Nitric oxide, NO2 = Nitrogen dioxide, SO2 = Sulphur dioxide, Org = Organic mass fraction, NH4 = Ammonium mass fraction, NO3 = Nitrates mass fraction, SO4 = Sulphates mass fraction, Cl = Chloride mass fraction, CN3 = Condensation Nuclei >3nm. Note how there does not seem to be any significant SO_2 or NO_2 pollution prior to the NPF start. At the same time of the particle growth there are enhancements in the organic, sulphate and ammonium mass

https://doi.org/10.5194/egusphere-2024-2062
Preprint. Discussion started: 22 July 2024

fraction. There are two events in this plot. One in the morning with an unknown start and the other at night. The first black line represents the NPF approximated ending time of a morning event. The light green vertical line marks the NPF approximated starting time of the nighttime event. The black line represents the NPF approximated ending time.

Like isoprene, the availability of monoterpene in the morning may determine how fast a NPF event can occur after SO_2 reaches the site. Monoterpenes are quickly oxidized by OH with relative short lifetimes compared to isoprene (Atkinson, 2000; Atkinson and Arey, 2003). Oxidized monoterpenes through the OH pathway favour OVOCs that eventually condense faster than isoprene oxidation products (Heinritzi et al., 2020; Link et al., 2021). With these events starting in the morning ~8:00 to 9:00, there will be enough monoterpenes available for a fast oxidation once the OH starts to build up in the atmosphere, and these OVOCs are easily condensed on already formed seeds or under acidic conditions.

The availability of monoterpene and SO_2 together may act as a catalyzer for faster particle formation compared to events with no monoterpenes, or events that start later in the day (noon) due to the absence of SO_2 at the site. In the absence of monoterpenes but presence isoprene the particle formation may be of smaller magnitude and the formation may occur at a slower rate. Isoprene oxidises mainly through the OH path to more stable compounds; usually MACR and MVK are used as tracers to determine which path and under what conditions isoprene is oxidised. MACR is oxidised to heavier OVOCs that eventually condense. Given that the PTR-ToF-MS does not separate these two compounds it is not possible to identify when changes between ratios of MACR to MVK are significant in the NPF events on the current dataset. In general, when there are not enough VOCs in the atmosphere the nucleation and growth will be slow or might not happen at all.

3.5 Night-time NPF Events

The main factor influencing the night-time events appears to be NO_2 pollution in the atmosphere during the night, however the data available for this study does not provide enough information to make a more definitive statement. Unfortunately, the NO_x instrument was not ideal for this type of measurement given that is not designed to be accurate at the low NO_x levels in rural areas; it is not capable of separating NO_x from NO_y and it was set up to calibrate in the night hours between 1:00 and 2:00 every day. Nonetheless, during the night events the particle size distribution data and the CN_3 captured particle formation and growth from nucleation to Aitken mode when there were considerable increases of NO_2, but the PM_1 aerosol mass showed a minimal increase at the same time (e.g. event during night of Feb 5th shown in Figure 8). This suggest that there are conditions to initiate the particle formation process but the conditions to increase the size/mass of the particles are not present at these times.

https://doi.org/10.5194/egusphere-2024-2062
Preprint. Discussion started: 22 July 2024

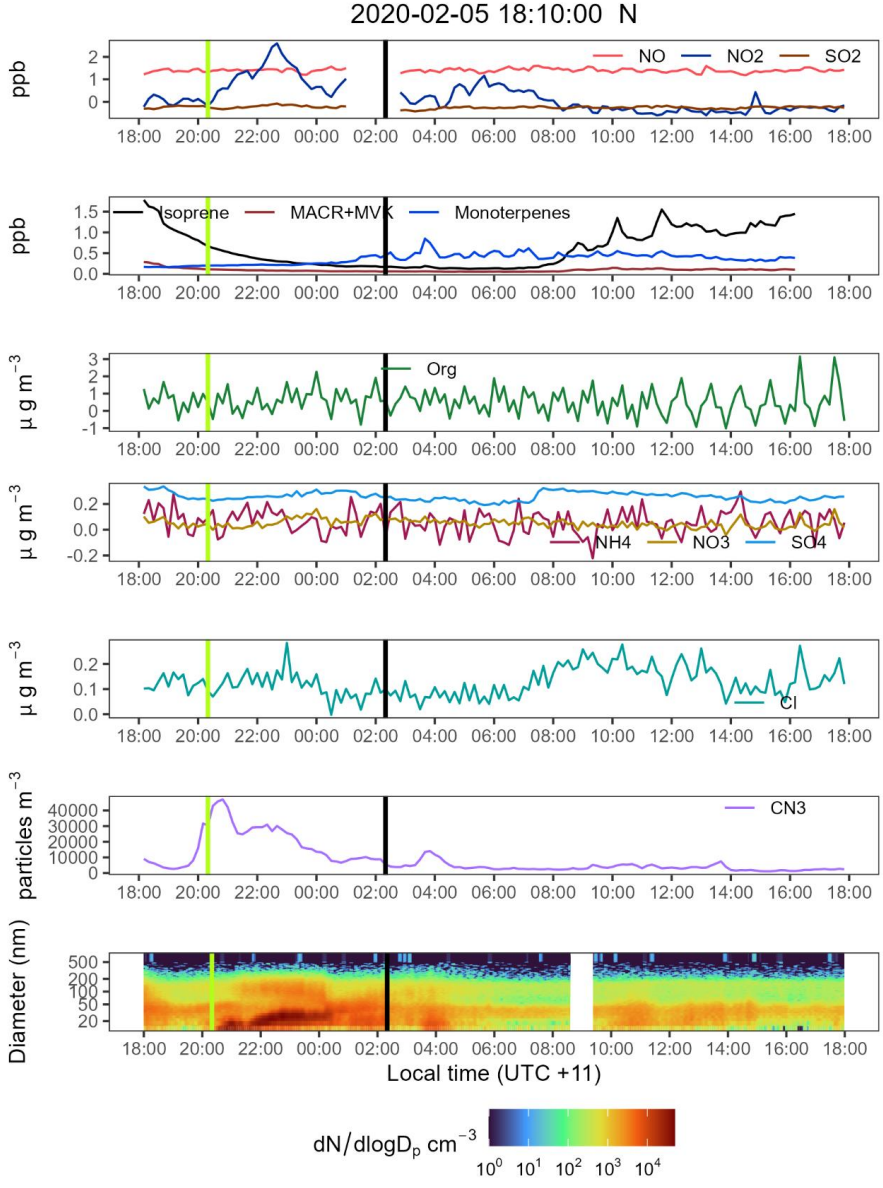

Figure 8: Time series of all selected variables during the NPF event during 2020-02-05. NO = Nitric oxide, NO2 = Nitrogen dioxide, SO2 = Sulphur dioxide, MACR+MVK = isoprene ox. products methacrolein and methyl-vinyl-ketone, Org = Organic mass fraction, NH4 = Ammonium mass fraction, NO3 = Nitrates mass fraction, SO4 = Sulphates mass fraction, Cl = Chloride mass fraction, CN3 = Condensation Nuclei >3nm. Note how the particle number goes below 10000 after the growth reached Aitken mode (0:00). There is not a substantial increase in the aerosol mass when the particle number and geometrical particle diameter increase. The light green vertical line marks the NPF approximated starting time of the nighttime event. The black line represents the NPF approximated ending time.

https://doi.org/10.5194/egusphere-2024-2062
Preprint. Discussion started: 22 July 2024

Another factor possibly influencing the NPF events at night may include the early night VOC accumulation in the residual planetary boundary layer. This might enhance particle formation for short periods of time, inducing nucleation and clusters, but not growth (due to the lack of VOCs once the available mass has reacted or condensed over existing particle seeds). This might explain the increase in particle number and density, but the relatively low mass observed during the night of Feb 23 compared to day-time events (see Figure 9).

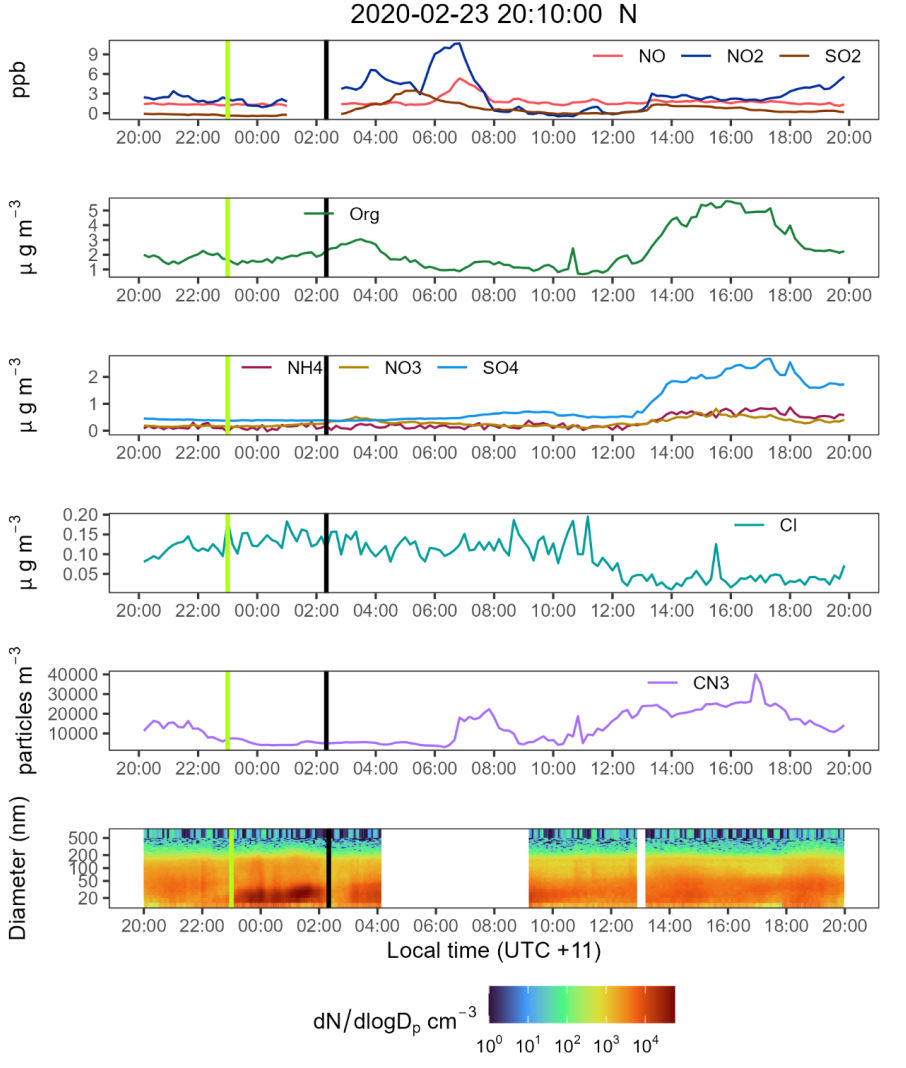

Figure 9: Time series of all selected variables during the NPF event during 2020-02-23. NO = Nitric oxide, NO2 = Nitrogen dioxide, SO2 = Sulphur dioxide, Org = Organic mass fraction, NH4 = Ammonium mass fraction, NO3 = Nitrates mass fraction, SO4 = Sulphates mass fraction, Cl = Chloride mass fraction, CN3 = Condensation Nuclei >3nm. The light green vertical line marks the NPF approximated starting time of the

https://doi.org/10.5194/egusphere-2024-2062
Preprint. Discussion started: 22 July 2024

nighttime event. The black line represents the NPF approximated ending time. There is a slight increase in the organic fraction while the event takes place. The organic fraction increases later that morning but there is not particle size distribution data to compare that period.

3.6 Aerosol fraction: Day vs Night

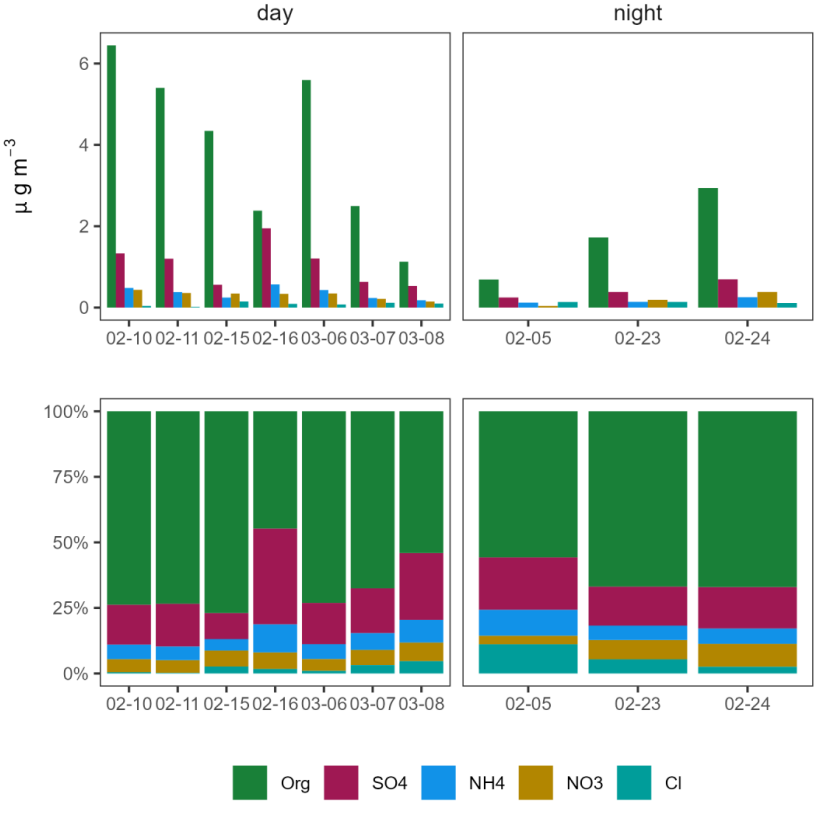

Figure 10: Average mass for each chemical group and event on the top panels. The bottom panel presents the percentage contribution to the mass of each of those fractions based on the average value presented above. Org = Organics; SO4 = sulphates; NH4 = ammonium; NO3 = nitrates and Cl = chlorides.

Figure 10 shows the mass fraction of the PM_1 aerosol mass measured in the ACSM. Most of the daytime events show a similar mass fraction distribution. The organic fraction is the largest mass fraction followed by sulphates, ammonium, nitrates, and chlorides. We observed higher sulphate mass fractions in days with higher SO_2 availability like the events on Feb 16th and March 8th, where the average sulphate mass fraction was larger or similar to the organic fraction (see Figure 10). These two events also display the highest proportion of ammonium during daytime events. The overall mass during night-time is much lower than during daytime, likely related to the lower concentrations of VOCs available during the night. Even with less total mass during the night, the contribution of each fraction is similar to the daytime events. The most notable difference between the mass fractions during day and nighttime NPF events is the higher fraction of

https://doi.org/10.5194/egusphere-2024-2062
Preprint. Discussion started: 22 July 2024

chlorides during night-time events likely driven by a greater relative contribution from sea salt to the aerosol mass.

Something to highlight is the higher fraction of ammonium compared to nitrates through all the events. Regions with low NO_x have been previously characterized with higher ammonium fractions compared to nitrates (Du et al., 2015; Liu et al., 2022; Petit et al., 2015; Takami et al., 2005; Topping et al., 2004), whilst regions with higher NO_x concentrations favour nitrate formation (Hu et al., 2015; Parworth et al., 2015; Poulain et al., 2020; Schlag et al., 2016). The local difference in relative mass composition is evident when comparing this study with the aerosol mass fractions observed in an urban site in Sydney (Keywood et al., 2016) in which high nitrate fractions were observed during most of the campaign.

4. Summary and Conclusions

Here we present aerosol concentration and composition data, VOCs and air pollutant concentrations collected during part of the COALA-2020 campaign including data from 5th Feb to 17th March at a rural site south of Sydney Australia. This period followed the Black Summer fires after heavy rainfall cleared the smoke, offering insights into atmospheric processes under clean or pristine conditions.

The atmosphere during the sampling period was classified as highly reactive with some particle formation taking place on more than 50% of the sampling days with. Like previous studies, daytime NPF events were correlated with the arrival of anthropogenic plumes at the site, suggesting their role in initiating particle formation. The positive correlation between PM_1 aerosol mass and CN_3 with isoprene concentrations suggests a direct relationship between biogenic emissions and organic aerosol formation.

The change between gas to aerosol phase was indirectly analysed through the evaluation of the conditions leading to NPF events. This analysis showed how SO_2 and NO_x plumes impacting the site drove NPF. The particle growth rate was dependent on available VOCs in the atmosphere and OH availability, also enhanced during periods with higher relative humidity and multiple intrusions of SO_2 and NO_x plumes producing particles bigger than 100 nm.

Night-time events were correlated to NO_2, but the enviromental conditions changed between the few identified events limiting the ability to draw definitive conclusions.

The COALA-2020 campaign highlights the significant role of biogenic emissions, particularly isoprene, driving NPF in Southeast Australia. These findings contribute to a better understanding of local atmospheric chemistry and its potential impact on regional air quality and climate. However, longer-term observations are necessary to capture the full picture of seasonal variations and non-fire related extreme events.

Supplementary Materials:

Author Contributions:

The experiment design was made by Clare Paton-Walsh (Murphy) and Melita Keywood.

The data collection was done by Jack Simmons, Travis Naylor, Paton-Walsh (Murphy), Asher Mouat, Melita Keywood, Ruhi Humpries, Malcolm Possell and Jhonathan Ramirez-Gamboa.

The data processing to convert mass spectra to concentration of VOCs was done by Asher Mouat under the direction and supervision of Jennifer Kaiser.

The data analysis was done by Jhonathan Ramirez-Gamboa

https://doi.org/10.5194/egusphere-2024-2062
Preprint. Discussion started: 22 July 2024

The paper was written by Jhonathan Ramirez-Gamboa and Clare Paton-Walsh (Murphy).

Funding:

COALA-2020 was supported by Australia's National Environmental Science Program through the Clean Air and Urban Landscapes hub. Jhonathan Ramirez-Gamboa was supported during his PhD studies by a commonwealth funded University Post-Graduate Award at the University of Wollongong.

Data Availability Statement:

Data is available at PANGEA via the following links:

- VOCs: https://doi.org/10.1594/PANGAEA.927277Aerosol size distributions: https://doi.org/10.1594/PANGAEA.928853
- Condensations nuclei > 3 nm in diameter: https://doi.org/10.1594/PANGAEA.925555
- Cloud condensation nuclei: https://doi.org/10.1594/PANGAEA.928925
- Green-house gases: https://doi.org/10.1594/PANGAEA.927313
- Air Quality data: https://doi.org/10.1594/PANGAEA.929001
- Meteorological data: https://doi.org/10.1594/PANGAEA.928929

Acknowledgments:

We are grateful to all who contributed to the COALA-2020 campaign. Particular thanks are due to all the staff at Cataract Scout Camp and research students and staff: Ian Galbally, Kathryn Emmerson, Gunashanhar Gunaratnam, John Kirkwood, Warren White, David Griffiths, Alex Carter, Alan Griffiths, Hamish McDougall and Graham Kettlewell.

Conflicts of Interest:

The authors declare no conflicts of interest.

References

ABARES: Australian forest profiles 2019: Eucalypt, Australian Bureau of Agricultural Resource Economics and Sciences (ABARES), 2019.

Annesi-Maesano, I., Baiz, N., Banerjee, S., Rudnai, P., Rive, S., and the, S. G.: Indoor Air Quality and Sources in Schools and Related Health Effects, J. Toxicol. Environ. Health Part B, 16, 491–550, https://doi.org/10.1080/10937404.2013.853609, 2013.

Atkinson, R.: Atmospheric chemistry of VOCs and NO(x), Atmos. Environ., 34, 2063–2101, https://doi.org/10.1016/S1352-2310(99)00460-4, 2000.

Atkinson, R. and Arey, J.: Gas-phase tropospheric chemistry of biogenic volatile organic compounds: a review, Atmos. Environ., 37, 197–219, https://doi.org/10.1016/S1352-2310(03)00391-1, 2003.

Au Yang, D., Bardoux, G., Assayag, N., Laskar, C., Widory, D., and Cartigny, P.: Atmospheric SO2 oxidation by NO2 plays no role in the mass independent sulfur isotope fractionation of urban aerosols, Atmos. Environ., 193, 109–117, https://doi.org/10.1016/j.atmosenv.2018.09.007, 2018.

Aydin, Y. M., Yaman, B., Koca, H., Dasdemir, O., Kara, M., Altiok, H., Dumanoglu, Y., Bayram, A., Tolunay, D., Odabasi, M., and Elbir, T.: Biogenic volatile organic compound (BVOC) emissions from forested areas in Turkey: Determination

https://doi.org/10.5194/egusphere-2024-2062
Preprint. Discussion started: 22 July 2024

of specific emission rates for thirty-one tree species, Sci. Total Environ., 490, 239–253, https://doi.org/10.1016/J.SCITOTENV.2014.04.132, 2014.

Chen, Z., Schofield, R., Rayner, P., Zhang, T., Liu, C., Vincent, C., Fiddes, S., Ryan, R. G., Alroe, J., Ristovski, Z. D., Humphries, R. S., Keywood, M. D., Ward, J., Paton-Walsh, C., Naylor, T., and Shu, X.: Characterization of aerosols over the Great Barrier Reef: The influence of transported continental sources, Sci. Total Environ., 690, 426–437, https://doi.org/10.1016/j.scitotenv.2019.07.007, 2019.

Dal Maso, M., Kulmala, M., Riipinen, I., and Wagner, R.: Formation and growth of fresh atmospheric aerosols: Eight years of aerosol size distribution data from SMEAR II, Hyytiälä, Finland, Boreal Environ. Res., 10, 323–336, 2005.

Du, W., Sun, Y. L., Xu, Y. S., Jiang, Q., Wang, Q. Q., Yang, W., Wang, F., Bai, Z. P., Zhao, X. D., and Yang, Y. C.: Chemical characterization of submicron aerosol and particle growth events at a national background site (3295 m a.s.l.) on the Tibetan Plateau, Atmospheric Chem. Phys., 15, 10811–10824, https://doi.org/10.5194/acp-15-10811-2015, 2015.

Emmerson, K., Possell, M., J. Aspinwall, M., Pfautsch, S., and G. Tjoelker, M.: Temperature response measurements from eucalypts give insight into the impact of Australian isoprene emissions on air quality in 2050, Atmospheric Chem. Phys., 20, 6193–6206, https://doi.org/10.5194/acp-20-6193-2020, 2020.

Emmerson, K. M., Galbally, I. E., Guenther, A. B., Paton-Walsh, C., Guerette, E.-A. A., Cope, M. E., Keywood, M. D., Lawson, S. J., Molloy, S. B., Dunne, E., Thatcher, M., Karl, T., and Maleknia, S. D.: Current estimates of biogenic emissions from eucalypts uncertain for southeast Australia, Atmospheric Chem. Phys., 16, 6997–7011, https://doi.org/10.5194/acp-16-6997-2016, 2016.

Emmerson, K. M., Cope, M. E., Galbally, I. E., Lee, S., and Nelson, P. F.: Isoprene and monoterpene emissions in south-east Australia: Comparison of a multi-layer canopy model with MEGAN and with atmospheric observations, Atmospheric Chem. Phys., 18, 7539–7556, https://doi.org/10.5194/acp-18-7539-2018, 2018.

Emmerson, K. M., Palmer, P. I., Thatcher, M., Haverd, V., and Guenther, A. B.: Sensitivity of isoprene emissions to drought over south-eastern Australia: Integrating models and satellite observations of soil moisture, Atmos. Environ., 209, 112–124, https://doi.org/10.1016/j.atmosenv.2019.04.038, 2019.

Fini, A., Brunetti, C., Loreto, F., Centritto, M., Ferrini, F., and Tattini, M.: Isoprene responses and functions in plants challenged by environmental pressures associated to climate change, Front. Plant Sci., 8, https://doi.org/10.3389/fpls.2017.01281, 2017.

Friedman, B. and Farmer, D.: SOA and gas phase organic acid yields from the sequential photooxidation of seven monoterpenes, Atmos. Environ., 187, https://doi.org/10.1016/j.atmosenv.2018.06.003, 2018.

Fry, J. L., Brown, S. S., Middlebrook, A. M., Edwards, P. M., Campuzano-Jost, P., Day, D. A., Jimenez, J. L., Allen, H. M., Ryerson, T. B., Pollack, I., Graus, M., Warneke, C., de Gouw, J. A., Brock, C. A., Gilman, J., Lerner, B. M., Dubé, W. P., Liao, J., and Welti, A.: Secondary organic aerosol (SOA) yields from NO3 radical + isoprene based on nighttime aircraft power plant plume transects, Atmospheric Chem. Phys., 18, 11663–11682, https://doi.org/10.5194/acp-18-11663-2018, 2018.

https://doi.org/10.5194/egusphere-2024-2062
Preprint. Discussion started: 22 July 2024

Guenther, A., Jiang, X., Heald, C. L., Sakulyanontvittaya, T., Duhl, T., Emmons, L. K., and Wang, X.: The Model of Emissions of Gases and Aerosols from Nature version 2.1 (MEGAN2.1): an extended and updated framework for modeling biogenic emissions, Geosci. Model Dev., 5, 1471–1492, https://doi.org/10.5194/gmd-5-1471-2012, 2012.

Heinritzi, M., Dada, L., Simon, M., Stolzenburg, D., Wagner, A. C., Fischer, L., Ahonen, L. R., Amanatidis, S., Baalbaki, R., Baccarini, A., Bauer, P. S., Baumgartner, B., Bianchi, F., Brilke, S., Chen, D., Chiu, R., Dias, A., Dommen, J., Duplissy, J., Finkenzeller, H., Frege, C., Fuchs, C., Garmash, O., Gordon, H., Granzin, M., El Haddad, I., He, X., Helm, J., Hofbauer, V., Hoyle, C. R., Kangasluoma, J., Keber, T., Kim, C., Kürten, A., Lamkaddam, H., Laurila, T. M., Lampilahti, J., Lee, C. P., Lehtipalo, K., Leiminger, M., Mai, H., Makhmutov, V., Manninen, H. E., Marten, R., Mathot, S., Mauldin, R. L., Mentler, B., Molteni, U., Müller, T., Nie, W., Nieminen, T., Onnela, A., Partoll, E., Passananti, M., Petäjä, T., Pfeifer, J., Pospisilova, V., Quéléver, L. L. J., Rissanen, M. P., Rose, C., Schobesberger, S., Scholz, W., Scholze, K., Sipilä, M., Steiner, G., Stozhkov, Y., Tauber, C., Tham, Y. J., Vazquez-Pufleau, M., Virtanen, A., Vogel, A. L., Volkamer, R., Wagner, R., Wang, M., Weitz, L., Wimmer, D., Xiao, M., Yan, C., Ye, P., Zha, Q., Zhou, X., Amorim, A., Baltensperger, U., Hansel, A., Kulmala, M., Tomé, A., Winkler, P. M., Worsnop, D. R., Donahue, N. M., Kirkby, J., and Curtius, J.: Molecular understanding of the suppression of new-particle formation by isoprene, Atmospheric Chem. Phys., 20, 11809–11821, https://doi.org/10.5194/acp-20-11809-2020, 2020.

Hu, W. W., Campuzano-Jost, P., Palm, B. B., Day, D. A., Ortega, A. M., Hayes, P. L., Krechmer, J. E., Chen, Q., Kuwata, M., Liu, Y. J., de Sá, S. S., McKinney, K., Martin, S. T., Hu, M., Budisulistiorini, S. H., Riva, M., Surratt, J. D., St. Clair, J. M., Isaacman-Van Wertz, G., Yee, L. D., Goldstein, A. H., Carbone, S., Brito, J., Artaxo, P., de Gouw, J. A., Koss, A., Wisthaler, A., Mikoviny, T., Karl, T., Kaser, L., Jud, W., Hansel, A., Docherty, K. S., Alexander, M. L., Robinson, N. H., Coe, H., Allan, J. D., Canagaratna, M. R., Paulot, F., and Jimenez, J. L.: Characterization of a real-time tracer for isoprene epoxydiols-derived secondary organic aerosol (IEPOX-SOA) from aerosol mass spectrometer measurements, Atmospheric Chem. Phys., 15, 11807–11833, https://doi.org/10.5194/acp-15-11807-2015, 2015.

Hussein, T., Dal Maso, M., Petäjä, T., Koponen, I., Paatero, P., Aalto, P., Hämeri, K., and Kulmala, M.: Evaluation of an automatic algorithm for fitting the particle number size distribution, Boreal Environ. Res., 10, 337–355, 2005.

Kalkavouras, P., Bougiatioti, A., Grivas, G., Stavroulas, I., Kalivitis, N., Liakakou, E., Gerasopoulos, E., Pilinis, C., and Mihalopoulos, N.: On the regional aspects of new particle formation in the Eastern Mediterranean: A comparative study between a background and an urban site based on long term observations, Atmospheric Res., 239, 104911, https://doi.org/10.1016/j.atmosres.2020.104911, 2020.

Kari, E., Hao, L., Ylisirniö, A., Buchholz, A., Leskinen, A., Yli-Pirilä, P., Nuutinen, I., Kuuspalo, K., Jokiniemi, J., Faiola, C. L., Schobesberger, S., and Virtanen, A.: Potential dual effect of anthropogenic emissions on the formation of biogenic secondary organic aerosol (BSOA), Atmospheric Chem. Phys., 19, 15651–15671, https://doi.org/10.5194/acp-19-15651-2019, 2019.

Kerminen, V.-M., Paramonov, M., Anttila, T., Riipinen, I., Fountoukis, C., Korhonen, H., Asmi, E., Laakso, L., Lihavainen, H., Swietlicki, E., Svenningsson, B., Asmi, A., Pandis, S. N., Kulmala, M., and Petäjä, T.: Cloud condensation nuclei production associated with atmospheric nucleation: a synthesis based on existing literature and new results, Atmospheric Chem. Phys., 12, 12037–12059, https://doi.org/10.5194/acp-12-12037-2012, 2012.

https://doi.org/10.5194/egusphere-2024-2062
Preprint. Discussion started: 22 July 2024

Keywood, M., Selleck, P., Galbally, I., Lawson, S., Powell, J., Cheng, M., Gillett, R., Ward, J., Harnwell, J., Dunne, E., Boast, K., Reisen, F., Molloy, S., Griffiths, A., Chambers, S., Humphries, R., Guerette, E.-A., Cohen, D. (2016):, Crumeyrolle, S., Zhang, C., Zeng, J., and Fedele, R.: Sydney Particle Study 2 - Aerosol and gas data collection. v1., edited by: CSIRO, , https://doi.org/10.4225/08/57903B83D6A5D, 2016.

Kiendler-Scharr, A., Wildt, J., Maso, M. D., Hohaus, T., Kleist, E., Mentel, T. F., Tillmann, R., Uerlings, R., Schurr, U., and Wahner, A.: New particle formation in forests inhibited by isoprene emissions, Nature, 461, 381–384, 2009.

Kroll, J. H., Ng, N. L., Murphy, S. M., Flagan, R. C., and Seinfeld, J. H.: Secondary Organic Aerosol Formation from Isoprene Photooxidation, Environ. Sci. Technol., 40, 1869–1877, https://doi.org/10.1021/es0524301, 2006.

Kulmala, M., Maso, M. D., Mäkelä, J. M., Pirjola, L., Väkevä, M., Aalto, P., Miikkulainen, P., Hämeri, K., and O'dowd, C. D.: On the formation, growth and composition of nucleation mode particles, Tellus B, 53, 479–490, https://doi.org/10.1034/j.1600-0889.2001.530411.x, 2001.

Link, M. F., Brophy, P., Fulgham, S. R., Murschell, T., and Farmer, D. K.: Isoprene versus Monoterpenes as Gas-Phase Organic Acid Precursors in the Atmosphere, ACS Earth Space Chem., 5, 1600–1612, https://doi.org/10.1021/acsearthspacechem.1c00093, 2021.

Liu, J., D'Ambro, E. L., Lee, B. H., Lopez-Hilfiker, F. D., Zaveri, R. A., Rivera-Rios, J. C., Keutsch, F. N., Iyer, S., Kurten, T., Zhang, Z., Gold, A., Surratt, J. D., Shilling, J. E., and Thornton, J. A.: Efficient Isoprene Secondary Organic Aerosol Formation from a Non-IEPOX Pathway, Environ. Sci. Technol., 50, 9872–9880, https://doi.org/10.1021/acs.est.6b01872, 2016a.

Liu, X., Zhu, H., Hu, Y., Feng, S., Chu, Y., Wu, Y., Wang, C., Zhang, Y., Yuan, Z., and Lu, Y.: Public's Health Risk Awareness on Urban Air Pollution in Chinese Megacities: The Cases of Shanghai, Wuhan and Nanchang, Int. J. Environ. Res. Public. Health, 13, 845, 2016b.

Liu, Z., Chen, H., Li, L., Xie, G., Ouyang, H., Tang, X., Ju, R., Li, B., Zhang, R., and Chen, J.-M.: Real-time single particle characterization of oxidized organic aerosols in the East China Sea, Npj Clim. Atmospheric Sci., 5, 47, https://doi.org/10.1038/s41612-022-00267-1, 2022.

Long, B., Bao, J., and Truhlar, D.: Reaction of SO2 with OH in the Atmosphere, Phys Chem Chem Phys, 19, https://doi.org/10.1039/C7CP00497D, 2017.

Mahilang, M., Deb, M. K., and Pervez, S.: Biogenic secondary organic aerosols: A review on formation mechanism, analytical challenges and environmental impacts, Chemosphere, 262, 127771, https://doi.org/10.1016/j.chemosphere.2020.127771, 2021.

Margitan, J. J.: Mechanism of the atmospheric oxidation of sulfur dioxide. Catalysis by hydroxyl radicals, J. Phys. Chem., 88, 3314–3318, https://doi.org/10.1021/j150659a035, 1984.

Mouat, A. P., Paton-Walsh, C., Simmons, J. B., Ramirez-Gamboa, J., Griffith, D. W. T., and Kaiser, J.: Measurement report: Observations of long-lived volatile organic compounds from the 2019–2020 Australian wildfires during the COALA campaign, Atmospheric Chem. Phys., 22, 11033–11047, https://doi.org/10.5194/acp-22-11033-2022, 2022.

https://doi.org/10.5194/egusphere-2024-2062
Preprint. Discussion started: 22 July 2024

Nestorowicz, K., Jaoui, M., Rudzinski, K. J., Lewandowski, M., Kleindienst, T. E., Spólnik, G., Danikiewicz, W., and Szmigielski, R.: Chemical composition of isoprene SOA under acidic and non-acidic conditions: effect of relative humidity, Atmospheric Chem. Phys., 18, 18101–18121, https://doi.org/10.5194/acp-18-18101-2018, 2018.

Ng, N. L., Kroll, J. H., Keywood, M. D., Bahreini, R., Varutbangkul, V., Flagan, R. C., Seinfeld, J. H., Lee, A., and Goldstein, A. H.: Contribution of First- versus Second-Generation Products to Secondary Organic Aerosols Formed in the Oxidation of Biogenic Hydrocarbons, Environ. Sci. Technol., 40, 2283–2297, https://doi.org/10.1021/es052269u, 2006.

Ng, N. L., Kwan, A. J., Surratt, J. D., Chan, A. W. H., Chhabra, P. S., Sorooshian, A., Pye, H. O. T., Crounse, J. D., Wennberg, P. O., Flagan, R. C., and Seinfeld, J. H.: Secondary organic aerosol (SOA) formation from reaction of isoprene with nitrate radicals (NO3), Atmospheric Chem. Phys., 8, 4117–4140, https://doi.org/10.5194/acp-8-4117-2008, 2008.

Nie, W., Yan, C., Yang, L., Roldin, P., Liu, Y., Vogel, A. L., Molteni, U., Stolzenburg, D., Finkenzeller, H., Amorim, A., Bianchi, F., Curtius, J., Dada, L., Draper, D. C., Duplissy, J., Hansel, A., He, X.-C., Hofbauer, V., Jokinen, T., Kim, C., Lehtipalo, K., Nichman, L., Mauldin, R. L., Makhmutov, V., Mentler, B., Mizelli-Ojdanic, A., Petäjä, T., Quéléver, L. L. J., Schallhart, S., Simon, M., Tauber, C., Tomé, A., Volkamer, R., Wagner, A. C., Wagner, R., Wang, M., Ye, P., Li, H., Huang, W., Qi, X., Lou, S., Liu, T., Chi, X., Dommen, J., Baltensperger, U., El Haddad, I., Kirkby, J., Worsnop, D., Kulmala, M., Donahue, N. M., Ehn, M., and Ding, A.: NO at low concentration can enhance the formation of highly oxygenated biogenic molecules in the atmosphere, Nat. Commun., 14, 3347, https://doi.org/10.1038/s41467-023-39066-4, 2023.

Ormeño, E., Mévy, J. P., Vila, B., Bousquet-Mélou, A., Greff, S., Bonin, G., and Fernandez, C.: Water deficit stress induces different monoterpene and sesquiterpene emission changes in Mediterranean species. Relationship between terpene emissions and plant water potential, Chemosphere, 67, 276–284, https://doi.org/10.1016/J.CHEMOSPHERE.2006.10.029, 2007.

Padhy, P. K. K. and Varshney, C. K. K.: Emission of volatile organic compounds (VOC) from tropical plant species in India, Chemosphere, 59, 1643–1653, 2005.

Parworth, C., Fast, J., Mei, F., Shippert, T., Sivaraman, C., Tilp, A., Watson, T., and Zhang, Q.: Long-term measurements of submicrometer aerosol chemistry at the Southern Great Plains (SGP) using an Aerosol Chemical Speciation Monitor (ACSM), Atmos. Environ., 106, 43–55, https://doi.org/10.1016/j.atmosenv.2015.01.060, 2015.

Paton-Walsh, C., Rayner, P., Simmons, J., Fiddes, S. L., Schofield, R., Bridgman, H., Beaupark, S., Broome, R., Chambers, S. D., Chang, L. T.-C., Cope, M., Cowie, C. T., Desservettaz, M., Dominick, D., Emmerson, K., Forehead, H., Galbally, I. E., Griffiths, A., Guérette, É.-A., Haynes, A., Heyworth, J., Jalaludin, B., Kan, R., Keywood, M., Monk, K., Morgan, G. G., Nguyen Duc, H., Phillips, F., Popek, R., Scorgie, Y., Silver, J. D., Utembe, S., Wadlow, I., Wilson, S. R., and Zhang, Y.: A Clean Air Plan for Sydney: An Overview of the Special Issue on Air Quality in New South Wales, Atmosphere, 10, 774, 2019.

Paton-Walsh, C., Emmerson, K. M., Garland, R. M., Keywood, M., Hoelzemann, J. J., Huneeus, N., Buchholz, R. R., Humphries, R. S., Altieri, K., Schmale, J., Wilson, S. R., Labuschagne, C., Kalisa, E., Fisher, J. A., Deutscher, N. M., van Zyl, P. G., Beukes, J. P., Joubert, W., Martin, L., Mkololo, T., Barbosa, C., de Fatima Andrade, M., Schofield, R., Mallet,

https://doi.org/10.5194/egusphere-2024-2062
Preprint. Discussion started: 22 July 2024

M. D., Harvey, M. J., Formenti, P., Piketh, S. J., and Olivares, G.: Key challenges for tropospheric chemistry in the Southern Hemisphere, Elem. Sci. Anthr., 10, 00050, https://doi.org/10.1525/elementa.2021.00050, 2022.

Petit, J.-E., Favez, O., Sciare, J., Crenn, V., Sarda-Estève, R., Bonnaire, N., Močnik, G., Dupont, J.-C., Haeffelin, M., and Leoz-Garziandia, E.: Two years of near real-time chemical composition of submicron aerosols in the region of Paris using an Aerosol Chemical Speciation Monitor (ACSM) and a multi-wavelength Aethalometer, ATMOSPHERIC Chem. Phys., 15, 2985–3005, https://doi.org/10.5194/acp-15-2985-2015, 2015.

Phillips, F. A., Naylor, T., Forehead, H., Griffith, D. W. T., Kirkwood, J., and Paton-Walsh, C.: Vehicle Ammonia Emissions Measured in An Urban Environment in Sydney, Australia, Using Open Path Fourier Transform Infra-Red Spectroscopy, Atmosphere, 10, 208, 2019.

Pope, C. A. and Dockery, D. W.: Health effects of fine particulate air pollution: Lines that connect, J. Air Waste Manag. Assoc., 56, 709–742, 2006.

Pöschl, U.: Atmospheric Aerosols: Composition, Transformation, Climate and Health Effects, Angew. Chem. Int. Ed., 44, 7520–7540, https://doi.org/10.1002/anie.200501122, 2005.

Poulain, L., Spindler, G., Grüner, A., Tuch, T., Stieger, B., van Pinxteren, D., Petit, J.-E., Favez, O., Herrmann, H., and Wiedensohler, A.: Multi-year ACSM measurements at the central European research station Melpitz (Germany) – Part 1: Instrument robustness, quality assurance, and impact of upper size cutoff diameter, Atmospheric Meas. Tech., 13, 4973–4994, https://doi.org/10.5194/amt-13-4973-2020, 2020.

Ren, Y., Qu, Z., Du, Y., Xu, R., Ma, D., Yang, G., Shi, Y., Fan, X., Tani, A., Guo, P., Ge, Y., and Chang, J.: Air quality and health effects of biogenic volatile organic compounds emissions from urban green spaces and the mitigation strategies, Environ. Pollut., 230, 849–861, https://doi.org/10.1016/j.envpol.2017.06.049, 2017.

Riva, M., Heikkinen, L., Bell, D. M., Peräkylä, O., Zha, Q., Schallhart, S., Rissanen, M. P., Imre, D., Petäjä, T., Thornton, J. A., Zelenyuk, A., and Ehn, M.: Chemical transformations in monoterpene-derived organic aerosol enhanced by inorganic composition, Npj Clim. Atmospheric Sci., 2, 2, https://doi.org/10.1038/s41612-018-0058-0, 2019.

Schlag, P., Kiendler-Scharr, A., Blom, M. J., Canonaco, F., Henzing, J. S., Moerman, M., Prévôt, A. S. H., and Holzinger, R.: Aerosol source apportionment from 1-year measurements at the CESAR tower in Cabauw, the Netherlands, Atmospheric Chem. Phys., 16, 8831–8847, https://doi.org/10.5194/acp-16-8831-2016, 2016.

Shi, L. H., Zanobetti, A., Kloog, I., Coull, B. A., Koutrakis, P., Melly, S. J., and Schwartz, J. D.: Low-Concentration PM2.5 and Mortality: Estimating Acute and Chronic Effects in a Population-Based Study, Environ. Health Perspect., 124, 46–52, https://doi.org/10.1289/ehp.1409111, 2016.

Simmons, J. B., Paton-Walsh, C., Mouat, A. P., Kaiser, J., Humphries, R. S., Keywood, M., Griffith, D. W. T., Sutresna, A., Naylor, T., and Ramirez-Gamboa, J.: Bushfire smoke plume composition and toxicological assessment from the 2019–2020 Australian Black Summer, Air Qual. Atmosphere Health, 15, 2067–2089, https://doi.org/10.1007/s11869-022-01237-5, 2022.

https://doi.org/10.5194/egusphere-2024-2062
Preprint. Discussion started: 22 July 2024

Smit, R., Kingston, P., Neale, D. W., Brown, M. K., Verran, B., and Nolan, T.: Monitoring on-road air quality and measuring vehicle emissions with remote sensing in an urban area, Atmos. Environ., 218, 116978, https://doi.org/10.1016/j.atmosenv.2019.116978, 2019.

Song, M., Zhang, C., Wu, H., Mu, Y., Ma, Z., Zhang, Y., Liu, J., and Li, X.: The influence of OH concentration on SOA formation from isoprene photooxidation, Sci. Total Environ., 650, 951–957, https://doi.org/10.1016/j.scitotenv.2018.09.084, 2019.

Stangl, C. M., Krasnomowitz, J. M., Apsokardu, M. J., Tiszenkel, L., Ouyang, Q., Lee, S., and Johnston, M. V.: Sulfur Dioxide Modifies Aerosol Particle Formation and Growth by Ozonolysis of Monoterpenes and Isoprene, J. Geophys. Res. Atmospheres, 124, 4800–4811, https://doi.org/10.1029/2018JD030064, 2019.

Takami, A., Miyoshi, T., Shimono, A., and Hatakeyama, S.: Chemical composition of fine aerosol measured by AMS at Fukue Island, Japan during APEX period, Atmos. Environ., 39, 4913–4924, https://doi.org/10.1016/j.atmosenv.2005.04.038, 2005.

Topping, D., Coe, H., McFiggans, G., Burgess, R., Allan, J., Alfarra, M. R., Bower, K., Choularton, T. W., Decesari, S., and Facchini, M. C.: Aerosol chemical characteristics from sampling conducted on the Island of Jeju, Korea during ACE Asia, Atmos. Environ., 38, 2111–2123, https://doi.org/10.1016/j.atmosenv.2004.01.022, 2004.

Uusitalo, H., Kontkanen, J., Ylivinkka, I., Ezhova, E., Demakova, A., Arshinov, M., Belan, B. D., Davydov, D., Ma, N., Petäjä, T., Wiedensohler, A., Kulmala, M., and Nieminen, T.: Occurrence of new particle formation events in Siberian and Finnish boreal forest, https://doi.org/10.5194/acp-2021-530, 2021.

Wang, J., Li, J., Ye, J., Zhao, J., Wu, Y., Hu, J., Liu, D., Nie, D., Shen, F., Huang, X., Huang, D. D., Ji, D., Sun, X., Xu, W., Guo, J., Song, S., Qin, Y., Liu, P., Turner, J. R., Lee, H. C., Hwang, S., Liao, H., Martin, S. T., Zhang, Q., Chen, M., Sun, Y., Ge, X., and Jacob, D. J.: Fast sulfate formation from oxidation of SO2 by NO2 and HONO observed in Beijing haze, Nat. Commun., 11, 2844, https://doi.org/10.1038/s41467-020-16683-x, 2020a.

Wang, X., Gemayel, R., Hayeck, N., Perrier, S., Charbonnel, N., Xu, C., Chen, H., Zhu, C., Zhang, L., Wang, L., Nizkorodov, S. A., Wang, X., Wang, Z., Wang, T., Mellouki, A., Riva, M., Chen, J., and George, C.: Atmospheric Photosensitization: A New Pathway for Sulfate Formation, Environ. Sci. Technol., 54, 3114–3120, https://doi.org/10.1021/acs.est.9b06347, 2020b.

Wang, Z., Zhang, C., Lv, G., Sun, X., Wang, N., and Li, Z.: Synergistic Reaction of SO2 with NO2 in Presence of H2O and NH3: A Potential Source of Sulfate Aerosol, Int. J. Mol. Sci., 20, 3746, https://doi.org/10.3390/ijms20153746, 2019.

Xu, L., Tsona, N. T., and Du, L.: Relative Humidity Changes the Role of SO2 in Biogenic Secondary Organic Aerosol Formation, J. Phys. Chem. Lett., 12, 7365–7372, https://doi.org/10.1021/acs.jpclett.1c01550, 2021.

Yu, F. and Luo, G.: Simulation of particle size distribution with a global aerosol model: contribution of nucleation to aerosol and CCN number concentrations, Atmospheric Chem. Phys., 9, 7691–7710, https://doi.org/10.5194/acp-9-7691-2009, 2009.

https://doi.org/10.5194/egusphere-2024-2062
Preprint. Discussion started: 22 July 2024

Zhang, H., Yee, L. D., Lee, B. H., Curtis, M. P., Worton, D. R., Isaacman-VanWertz, G., Offenberg, J. H., Lewandowski, M., Kleindienst, T. E., Beaver, M. R., Holder, A. L., Lonneman, W. A., Docherty, K. S., Jaoui, M., Pye, H. O. T., Hu, W., Day, D. A., Campuzano-Jost, P., Jimenez, J. L., Guo, H., Weber, R. J., de Gouw, J., Koss, A. R., Edgerton, E. S., Brune, W., Mohr, C., Lopez-Hilfiker, F. D., Lutz, A., Kreisberg, N. M., Spielman, S. R., Hering, S. V., Wilson, K. R., Thornton, J. A., and Goldstein, A. H.: Monoterpenes are the largest source of summertime organic aerosol in the southeastern United States, Proc. Natl. Acad. Sci., 115, 2038–2043, https://doi.org/10.1073/pnas.1717513115, 2018.